A 3D Finite-Volume Solver for Resin Flow in Fibrous Media: Advancing Simulations of the RTM Process

Hamza BOULLOUZ[1,3], Saturné Ayidegnon[1], Imad KISSAMI[1], Imad ELMAHI[1,2], Abdelghani SAOUAB[3]

[1] College of Computing, Mohammed VI Polytechnic University, Lot 660, Ben Guerir, 43150, Morocco
[2] ENSAO, LMCS, Complexe Universitaire, B.P. 669, 60000 Oujda, Morocco
[3] Normandie Univ, UNIHAVRE, CNRS, LOMC, 76600 Le Havre, France

June 12, 2025

Outlines

1 Introduction
2 Mathematical model: flow and filtration modeling
- Flow modeling

3 Numerical methods
4 Numerical results
5 Conclusions
6 Bibliography

Introduction

Composite Materials

A composite material combines at least two different materials, resulting in superior overall performance compared to the individual components.

Composite Materials

A composite material combines at least two different materials, resulting in superior overall performance compared to the individual components.

Benefits

- High strength and rigidity
- Low weight compared to a metal solution
- Good fatigue resistance
- Ability to dampen vibrations

Composite Materials

A composite material combines at least two different materials, resulting in superior overall performance compared to the individual components.

Benefits

- High strength and rigidity
- Low weight compared to a metal solution
- Good fatigue resistance
- Ability to dampen vibrations

Industrial Applications

- Automobile
- Aeronautics
- The nautical
- The railway
- General mechanics

Composite Materials

A composite material combines at least two different materials, resulting in superior overall performance compared to the individual components.

Benefits

- High strength and rigidity
- Low weight compared to a metal solution
- Good fatigue resistance
- Ability to dampen vibrations

Industrial Applications

- Automobile
- Aeronautics
- The nautical
- The railway
- General mechanics

Composite materials $\longrightarrow$ **Functional composites**

RTM (Resin Transfer Molding)

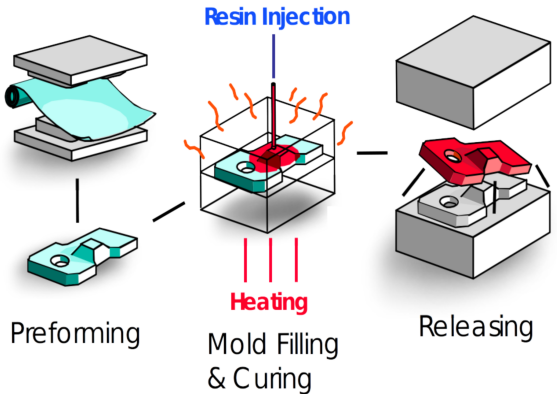

RTM (Resin Transfer Molding)

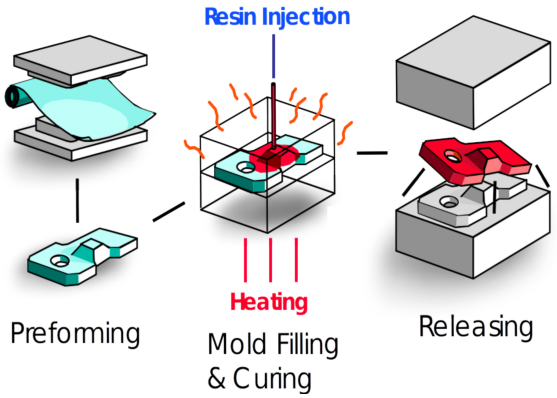

1. Developing composite processes through trial and error is expensive and slow.
2. Industry sees the advantages of using software simulations for prediction.
3. Simulations reduce costs and time compared to trial and error.

RTM (Resin Transfer Molding)

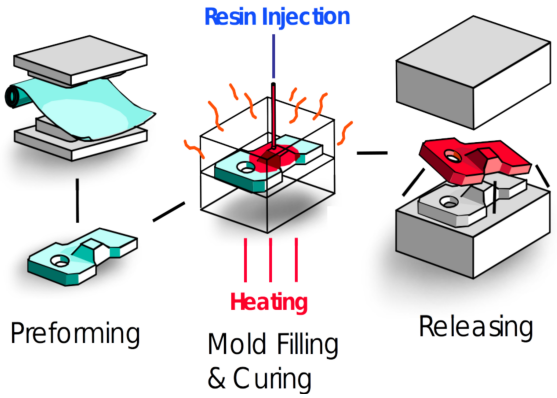

1. Developing composite processes through trial and error is expensive and slow.
2. Industry sees the advantages of using software simulations for prediction.
3. Simulations reduce costs and time compared to trial and error.

RTM (Resin Transfer Molding)

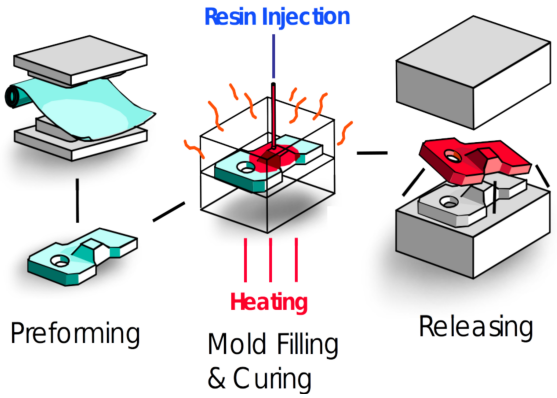

1. Developing composite processes through trial and error is expensive and slow.
2. Industry sees the advantages of using software simulations for prediction.
3. Simulations reduce costs and time compared to trial and error.

Mathematical model: flow and filtration modeling

Pressure equation - elliptic

Darcy's law:

$$U = -\frac{K}{\mu}\nabla P \tag{1}$$

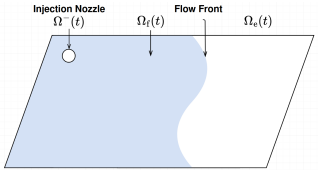

The continuity equation: $\mathrm{div}(U) = 0$

The governing equation of the pressure:

$$\boxed{\mathrm{div}\left(\frac{K}{\mu}\nabla P\right) = 0} \tag{2}$$

- K, μ, P, U: permeability, viscosity, pressure, velocity.

Pressure equation - elliptic

Darcy's law:

$$U = -\frac{K}{\mu}\nabla P \tag{1}$$

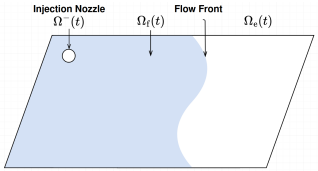

The continuity equation: $\mathrm{div}(U) = 0$

The governing equation of the pressure:

$$\boxed{\mathrm{div}\left(\frac{K}{\mu}\nabla P\right) = 0} \tag{2}$$

- K, μ, P, U: permeability, viscosity, pressure, velocity.

Saturation equation - hyperbolic

$$\boxed{\frac{\partial I}{\partial t} + U \cdot \nabla I = 0} \tag{3}$$

- The volume fraction, I, is defined as

$$I(\mathrm{x}, t) = \begin{cases} 1 & \text{if } \mathrm{x} \in \Omega_{\mathrm{f}}(t) \\ 0 & \text{if } \mathrm{x} \notin \Omega_{\mathrm{f}}(t) \end{cases}$$

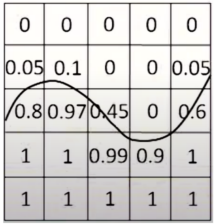

$\Omega_{\mathrm{f}}(t)$ represents the fluid domain at time t

$$\underbrace{-I(\mathrm{x})\,\mathrm{div}\left(\frac{K}{\mu}\nabla P\right)}_{\text{saturated domain}} + \underbrace{\alpha(I)(1-I(\mathrm{x}))P}_{\text{unsaturated domain}} = 0 \tag{4}$$

where $\alpha(I)$ is used in order to ensure dimensional homogeneity [1].

Numerical methods

Finite volume method: popular → multiphase flow equations in reservoir simulation

- Local conservation
- Geometrically flexible (tetrahedral meshes)

Discretization of the pressure equation in 3D

Notations:

- $\bar{\Omega} = \bigcup_{\mathcal{K}\in\mathcal{T}} \mathcal{K}$: domain decomposition
- $x_{\mathcal{K}}$: The center of the tetrahedron $\mathcal{K}$
- $|\mathcal{K}|$: The volume of the tetrahedron $\mathcal{K}$
- $|\Gamma|$: The area of the face Γ of $\mathcal{K}$
- $\epsilon_{\mathcal{K}}$: The set of faces Γ of $\mathcal{K}$
- $n_{\mathcal{K}\Gamma}$: Unit normal to face Γ outward from $\mathcal{K}$

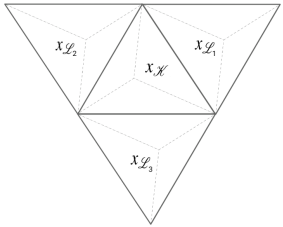

The integration of equation (4) over a tetrahedral control volume $\mathcal{K}$ gives:

$$-I_{\mathcal{K}} \sum_{\sigma\in\varepsilon_{\mathcal{K}}} \underbrace{\int_{\Gamma} \frac{K}{\mu} \nabla P \cdot n_{\mathcal{K}\Gamma}}_{\stackrel{\text{def}}{=} \bar{F}_{\mathcal{K},\Gamma}} + \alpha(I_{\mathcal{K}})(1 - I_{\mathcal{K}}) P_{\mathcal{K}} |\mathcal{K}| = 0 \qquad (5)$$

Pressure flux evaluation in 3D:

The divergence theorem is applied to the 3D diamond (dual) control volume $\mathcal{D}$ surrounding face Γ, leading to:

$$\nabla P|_{\Gamma} \approx \nabla_{\mathcal{D}}^{\mathcal{T}} P = \frac{1}{|\mathcal{D}|} \sum_{\epsilon \in \partial \mathcal{D}} P_{|_{\epsilon}} \int_{\epsilon} \mathrm{n}_{\epsilon} \, d\Gamma \qquad (6)$$

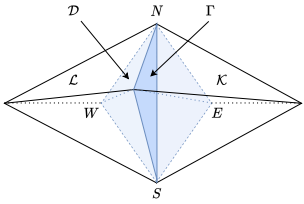

where ϵ are the polygonal faces of the polyhedral dual cell $\mathcal{D}$.

For a face ϵ shared by vertices N_1, N_2, and N_3, we approximate:

$$\nabla_{\mathcal{D}}^{\mathcal{T}} P \approx \frac{1}{|\mathcal{D}|} \sum_{\epsilon \in \partial \mathcal{D}} \left(\frac{1}{3} \sum_{i=1}^{N_3} P_{N_i} \right) \int_{\epsilon} \mathrm{n}_{\epsilon} \, d\Gamma \qquad (7)$$

Node pressures P_{N_i} are obtained through interpolation from neighboring cell centers.

Discretization of the advection equation in 3D

The advection equation, describing the transport of volume fraction I is discretized over tetrahedral control volumes as:

$$W_{\mathcal{K}}^{n+1} = W_{\mathcal{K}}^{n} - \frac{\Delta t}{|\mathcal{K}|} \sum_{\substack{\Gamma \subset \partial \mathcal{K} \\ \Gamma = (\mathcal{K}|\mathcal{L})}} |\Gamma| \cdot F(U \cdot \mathrm{n}_{\mathcal{K},\mathcal{L}}) \tag{8}$$

The flux $F(U \cdot \mathrm{n}_{\mathcal{K},\mathcal{L}})$ is computed using a second-order upwind scheme with the Barth-Jespersen limiter [2]:

$$F(U \cdot \mathrm{n}_{\mathcal{K},\mathcal{L}}) = \begin{cases} W_{\mathcal{K}} + \psi_{\mathcal{K}} \nabla W_{\mathcal{K}} \cdot \overrightarrow{r_{\mathcal{K}}} & \text{if } U \cdot \mathrm{n}_{\mathcal{K},\mathcal{L}} > 0 \\ W_{\mathcal{L}} + \psi_{\mathcal{L}} \nabla W_{\mathcal{L}} \cdot \overrightarrow{r_{\mathcal{L}}} & \text{otherwise} \end{cases} \tag{9}$$

- The vector $\overrightarrow{r_{\mathcal{K}}}$ points from the centroid of cell $\mathcal{K}$ to the centroid of the face Γ.
- Gradient reconstruction in 3D uses the diamond technique over tetrahedral neighbors.

Barth-Jespersen limiter in 3D

$$\psi_{\mathcal{K}} = \begin{cases} \min\left(1, \dfrac{W_{\max} - W_{\mathcal{K}}}{\nabla W_{\mathcal{K}} \cdot \overrightarrow{r_{\mathcal{K}}}}\right), & \text{if } \nabla W_{\mathcal{K}} \cdot \overrightarrow{r_{\mathcal{K}}} > 0 \\ 1, & \text{if } \nabla W_{\mathcal{K}} \cdot \overrightarrow{r_{\mathcal{K}}} = 0 \\ \min\left(1, \dfrac{W_{\min} - W_{\mathcal{K}}}{\nabla W_{\mathcal{K}} \cdot \overrightarrow{r_{\mathcal{K}}}}\right), & \text{if } \nabla W_{\mathcal{K}} \cdot \overrightarrow{r_{\mathcal{K}}} < 0 \end{cases} \tag{10}$$

where $W_{\max}$ and $W_{\min}$ are the maximum and minimum values of W among $\mathcal{K}$ and all its face-sharing neighbors.

CFL condition for 3D stability:

This scheme is conditionally stable if $Cr < 1$:

$$\Delta t = C_r \min_{\Gamma=(\mathcal{K},\mathcal{L})} \left(\frac{|\mathcal{K}| + |\mathcal{L}|}{2|\Gamma| \max_p |\lambda_p|_\Gamma} \right)$$

- Γ: shared face between tetrahedra $\mathcal{K}$ and $\mathcal{L}$
- $|\lambda_p|$: maximum eigenvalue (e.g., local velocity magnitude)

Numerical results

Validation against analytical solution: Unidirectional Injection

- **Setup:** Boundary and initial conditions (left), unstructured mesh (right)

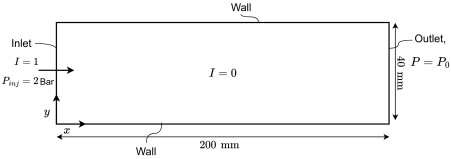

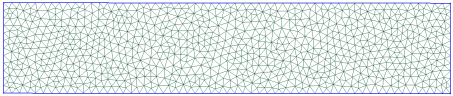

- **Simulation parameters:**

$$K = 2.65 \cdot 10^{-9}\,\mathbb{I}\,\mathrm{m}^2, \quad \mu = 0.109\,\mathrm{Pa{\cdot}s}, \quad \Phi = 0.7, \quad \alpha(I) = 2 \cdot 10^{-6}\,(\mathrm{Pa{\cdot}s})^{-1}, \quad \mathbb{I} = \begin{pmatrix} 1 & 0 \\ 0 & 1 \end{pmatrix}$$

- **Solution at time $t = 18$ s:**

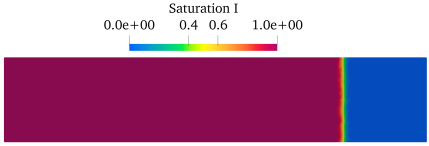

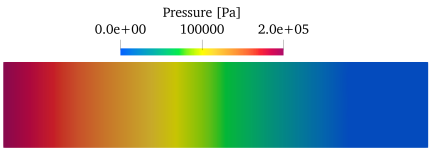

Validation against analytical solution: unidirectional injection

- Saturation profiles at four different time instants: t = 1, 5, 12, and 25 seconds

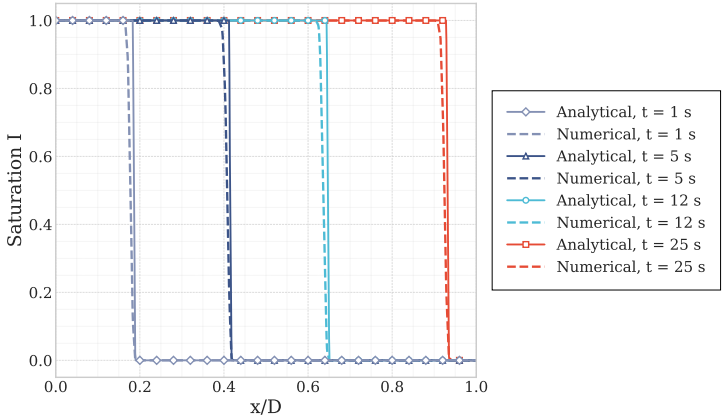

Validation against analytical solution: Unidirectional Injection

- **Pressure distribution**

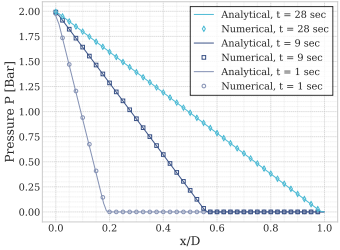

- **Flow front position over time**

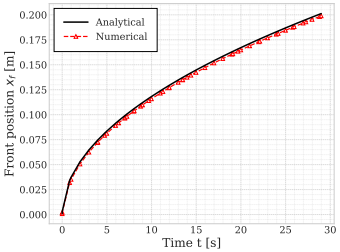

Table: Error Norms and CPU Time for 2D Mesh Refinement

Cells	**Nodes**	L_2 Norm	L_1 Norm	**CPU Time [s]**
996	551	4.40×10^{-4}	3.20×10^{-2}	4.57
1968	1059	2.84×10^{-4}	2.30×10^{-2}	10.15
4014	2113	1.62×10^{-4}	1.80×10^{-2}	28.16

Validation against analytical solution: Radial Injection

- **Setup:** Boundary and initial conditions (left), unstructured mesh (right)

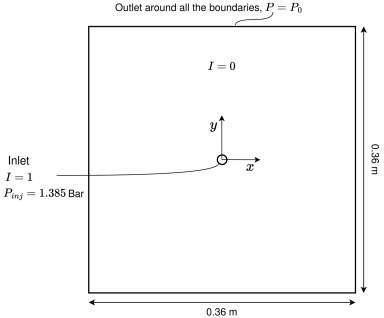

Geometry

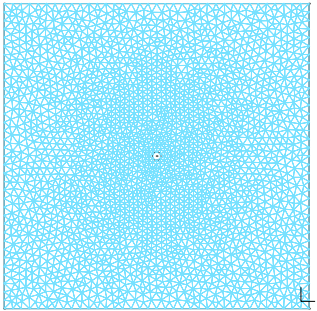

Unstructured Mesh

Validation against analytical solution: Unidirectional Injection

- **Simulation parameters:**

$$K = 2.55 \cdot 10^{-9}\,\mathbb{I}\,\mathrm{m}^2, \quad \mu = 0.11\,\mathrm{Pa{\cdot}s}, \quad \Phi = 0.79, \quad \alpha(I) = 2 \cdot 10^{-6}\,(\mathrm{Pa{\cdot}s})^{-1}$$

- **Solution at time $t = 4$ s:**

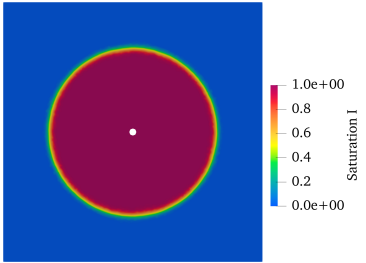

Volume Fraction

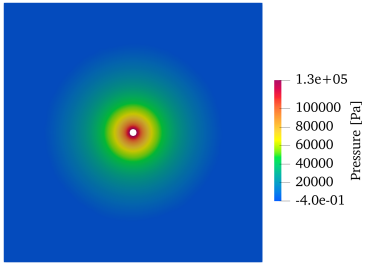

Pressure Field

Validation against analytical solution: Radial Injection

- **Pressure distribution**

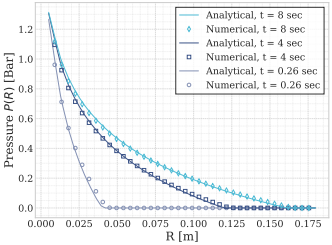

- **Flow front position vs. time**

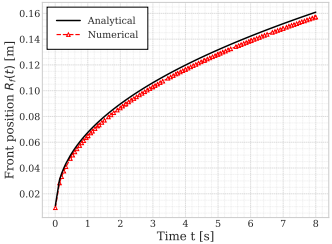

Table: Error Norms and CPU Time for Mesh Refinement – Radial Injection Case

Cells	**Nodes**	L_2 Norm	L_1 Norm	**CPU Time [s]**
4,022	2,078	1.40×10^{-3}	1.04×10^{-1}	96
8,034	4,122	9.43×10^{-4}	9.07×10^{-2}	414
15,892	8,096	5.48×10^{-4}	6.60×10^{-2}	810

3D Results: Unidirectional Injection

- **Setup:** This test case extends the first (2D) unidirectional injection to 3D, using the same physical parameters.
- The domain is discretized using unstructured tetrahedral elements.
- The numerical method demonstrates accurate front tracking and pressure field evolution in 3D.

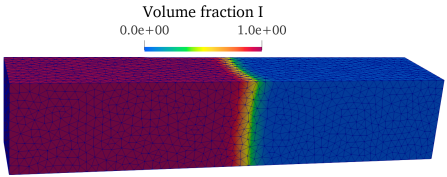

Volume Fraction (Front Location)

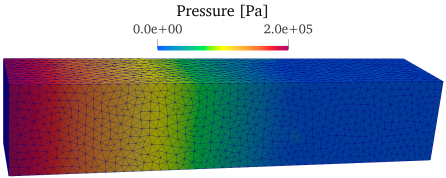

Pressure Field (Slice View)

The 3D solver shows consistent physical behavior and stable front propagation under the same boundary conditions.

Conclusions

- A **finite volume method** has been developed to simulate **resin flow** through porous media during the RTM process.
- The method has been **validated in 2D** using analytical solutions for both unidirectional and radial injection cases, confirming accuracy and convergence.
- The numerical approach has been **extended to 3D** using unstructured tetrahedral meshes, enabling realistic simulations of complex mold geometries.
- This work provides a reliable numerical foundation for **predicting and optimizing flow behavior** in composite manufacturing processes.

Merci de votre attention

References

[1] JA Garcıa, LI Gascón, and Francisco Chinesta. "A fixed mesh numerical method for modelling the flow in liquid composites moulding processes using a volume of fluid technique". In: *Computer methods in applied mechanics and engineering* 192.7-8 (2003), pp. 877–893.

[2] Imad Kissami. "Manapy: an MPI-based Python framework for solving Poisson's equation using finite volume on unstructured-grid". In: *AIP Conference Proceedings*. Vol. 3034. 1. AIP Publishing. 2024.